EMI Considerations in Selecting Heat-Sink-Thermal-Gasket Materials

Yu Huang, Joseph E. Butler, *Senior Member, IEEE*, Miksa de Sorgo, *Member, IEEE*, Richard E. DuBroff, *Senior Member, IEEE*, Todd H. Hubing, *Senior Member, IEEE*, James L. Drewniak, *Member, IEEE*, and Thomas P. Van Doren, *Senior Member, IEEE*

***Abstract*—Specific design criteria are proposed to mitigate radiated emissions from a resonant enclosure excited by a heat sink acting as a microstrip patch antenna source. In this particular application, the EMI mechanism is assumed to be due to coupling from the dominant TM^{z}_{010} mode to one or more resonant modes associated with the enclosure dimensions. The enclosure is then presumed to radiate, at the enclosure resonance frequencies, through one or more apertures, slots, or seams. The EMI-reduction strategy consists of shifting the resonant frequency of the dominant-patch antenna mode by dielectrically loading the patch antenna with thermal-gasket material having a specified electric permittivity. Specific formulas and graphs will be presented showing how to select the electric permittivity of the thermal-gasket material in order to obtain a given frequency shift. A comparison of experimental measurements with the predictions of the design criteria indicates that frequency shifts of up to approximately three times the bandwidth of the patch resonance can be predicted with reasonable accuracy. In at least two different commercial products that we are aware of, changing the electrically insulating heat sink gasket materials has solved specific radiated EMI problems.**

***Index Terms*—Electromagnetic interference, resonance, microstrip antenna.**

I. Introduction

EXPERIMENTAL data and testing [1] has shown that heat sinks can be an important part of the mechanism allowing CPU clock harmonics on a circuit board to radiate. Noise voltages generated on the circuit board can capacitively couple to the relatively large metal structure of a heat sink. If, as is customary, the heat sink is not well grounded, the heat sink and power or ground planes associated with the printed circuit boards can form an antenna resembling a microstrip patch antenna. Given an enclosure with sufficiently large slots, seams, or apertures a favorable coupling path can occur when a clock harmonic frequency closely matches both the resonant frequency of the heat sink-patch antenna structure and the resonant frequency of an enclosure mode.

Manuscript received December 21, 1999; revised March 5, 2001. This work was supported by the EMC Consortium at the University of Missouri, Rolla, MO.

Y. Huang was with the University of Missouri, Rolla, MO 65409-0249 USA. She is currently with Tegic Communications, Seattle, WA 98109 USA.

J. Butler and M. de Sorgo are with the Chomerics Division of Parker Hannifin Company, Woburn, MA 01888-4014 USA.

R. E. DuBroff, T. H. Hubing, J. L. Drewniak, and T. P. Van Doren are with the Department of Electrical and Computer Engineering, University of Missouri, Rolla, MO 65409-0249 USA.

Publisher Item Identifier S 0018-9375(01)07144-7.

As long as the physical dimensions of the enclosure are unchanged, the cavity-resonance frequencies should remain the same. However, as will be shown in the following sections, the introduction of thin layers of electrically nonconductive thermal gasket materials can produce significant and predictable shifts in the resonant frequency of the patch source.

The predicted frequency shifts are compared with experimental measurements for patch sources both in free space and in slotted metal enclosures having dimensions commensurate with desktop personal computers or workstations. For patch sources in enclosures, shifts in the patch-resonance frequency are often obscured by the presence of numerous cavity modes. In these cases, a cross-correlation method has been used to identify the frequency shift due to the presence of thermal gasket material.

The amount of frequency shift produced by the introduction of nonconductive materials can be significant when compared to the bandwidth of the patch source resonance. For this reason, a procedure for predicting the frequency shift to bandwidth ratio is developed and confirmed with experimental measurements. The predicted frequency shift to bandwidth ratio is then presented in a graphical form to assist designers in selecting (or changing) heat-sink gasket materials on the basis of electrical permittivity.

II. Experimental Results

An initial set of experimental measurements was performed to compare the calculated and measured frequency shifts produced when a microstrip patch antenna structure was loaded with various dielectrics. The patch structure for these initial measurements consisted of a 40 by 50 cm aluminum ground plane with an 8 by 8 cm square driven patch. The driven patch was constructed from copper tape and located 3.8 mm above the ground plane. The dielectric material was placed between the driven patch and the ground plane. A 50-Ω coaxial cable connected port 1 of a Wiltron 3724 A Network Analyzer, through a type-N connector, to the center of the driven patch. The feed point was at $x = 20$ cm and $y = 12.5$ cm for the coordinate system shown in Fig. 1. The inner conductor of the coaxial cable was extended by a thin wire, 0.16 cm in diameter, and attached to the driven patch while the outer conductor was connected to the ground plane. A horizontally-polarized receiving antenna was placed in the broadside direction relative to the patch antenna. The receiving antenna was connected to port 2 of the network analyzer, using another 50-Ω coaxial cable. The microstrip

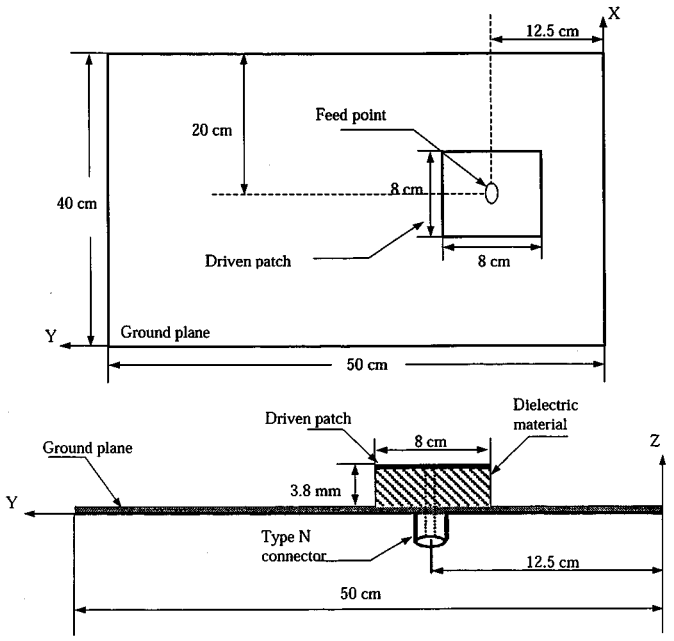

Fig. 1. Top and side views showing the dimensions of the patch antenna.

patch antenna and the receiving antenna were placed inside a shielded room to prevent contamination of the measurements from external radio frequency sources.

Eight different electrically nonconductive heat-sink gasket materials, having differing values of relative permittivity, were investigated. These materials were placed, one at a time, between the driven patch and the ground plane as shown by the region labeled "Dielectric material" in Fig. 1(b). Each of these test materials was in the form of one (or more) thin sheets. Due to the differing thicknesses of each sheet of material, the 3.8-mm space between the driven patch and the ground plane could not always be completely filled with the test material. In these cases, the space between the driven patch and the ground plane was filled partially with air ($\epsilon = \epsilon_0$) and partially with a sheet of dielectric material ($\epsilon = \epsilon_r \epsilon_0$). To compensate for this nonuniform dielectric, an effective relative permittivity was determined on the basis of an idealized parallel-plate capacitor having two dielectric slabs (one with $\epsilon = \epsilon_0$ and one with $\epsilon_0 = \epsilon_r \epsilon_0$). Letting a be the thickness of the gasket material and letting d be the separation between the driven patch and the ground plane (3.8 mm in this case) the effective relative permittivity can be defined as

$$\frac{\epsilon_{r,\text{effective}} \cdot \epsilon_0 \cdot s}{d} = \left(\frac{a}{\epsilon_r \cdot \epsilon_0 \cdot s} + \frac{b}{\epsilon_0 \cdot s} \right)^{-1} \tag{1}$$

where b is the thickness of the air layer ($b = d - a$) and s is the area of the driven patch. The effective relative permittivity is then

$$\epsilon_{r,\text{effective}} = \frac{d}{(a/\epsilon_r) + b}. \tag{2}$$

Fig. 2 shows, as one example, the swept frequency S_{11} parameter curve for a reference case, together with a curve for a thermal gasket material characterized by $\epsilon_r = 3.45$ and $\epsilon_{r,\text{effective}} = 1.45$. Without the thermal gasket material, there is a patch-source resonance at approximately 3.26 GHz. With the

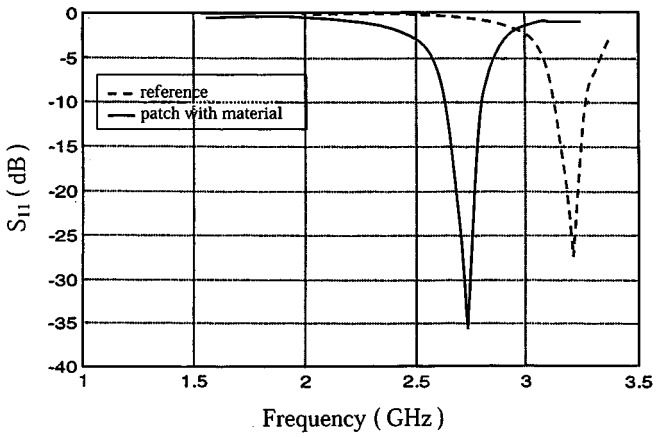

Fig. 2. The S_{11} characteristics of a patch source with (dark curve) and without (light curve) thermal gasket material.

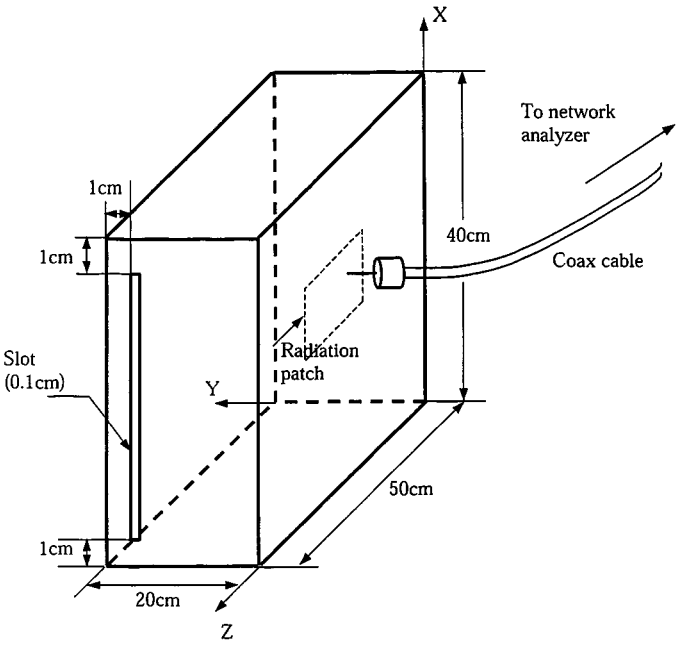

Fig. 3. Patch-antenna source incorporated into a slotted metal enclosure.

gasket material the patch resonance occurs at approximately 2.76 GHz. In short, as shown in Fig. 2 the patch resonance frequency shifts by an amount (approximately 500 MHz) that is significant when compared to the bandwidth of the resonance at either frequency.

For the next set of measurements, the patch antenna structure including the ground plane was incorporated as one wall of a slotted metal enclosure. Fig. 3 shows the dimensions of the enclosure and the slot. Again, S_{11} parameter curves were obtained for a reference case ($\epsilon_{r,\text{effective}} = 1.00$) and for the same thermal gasket material ($\epsilon_{r,\text{effective}} = 1.45$). The results of these measurements are shown in Fig. 4. In this case, any frequency shift between the upper and lower panels is well camouflaged by the presence of numerous cavity-mode resonances. These cavity-mode resonances are determined in turn by the physical dimensions of the enclosure through the relationship

$$f_{mnp} = \frac{c_0}{2\pi} \sqrt{\left(\frac{m\pi}{W}\right)^2 + \left(\frac{n\pi}{L}\right)^2 + \left(\frac{p\pi}{h}\right)^2} \tag{3}$$

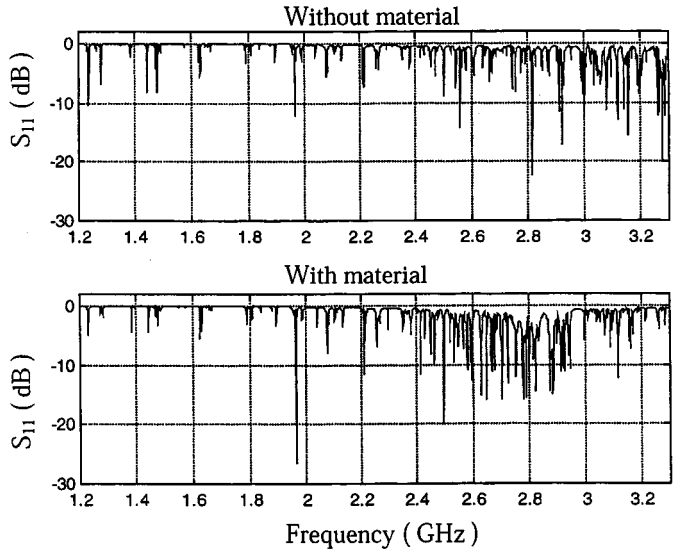

Fig. 4. The S_{11} characteristics of a patch source in an enclosure with (lower panel) and without (upper panel) thermal gasket material.

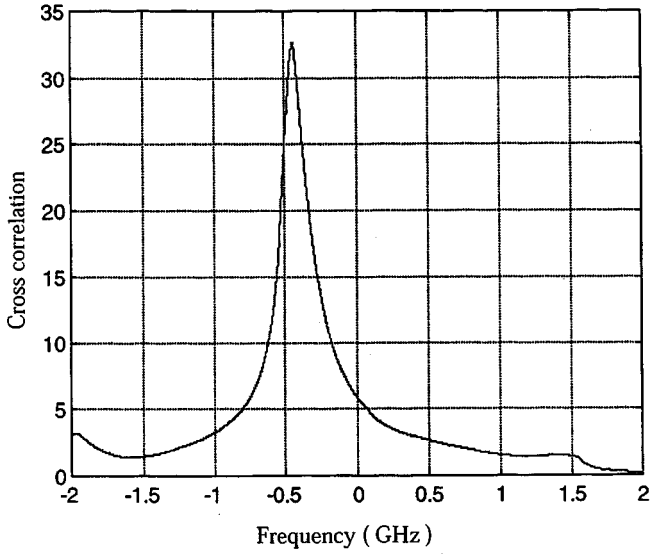

Fig. 5. Cross correlation between S_{11} curves for reference and dielectrically loaded patch sources in open space.

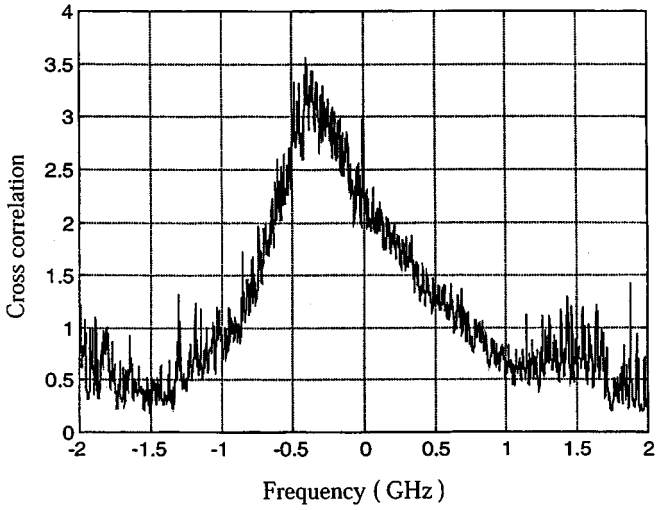

Fig. 6. Cross correlation between S_{11} curves for reference and dielectrically loaded patch sources in a slotted metal enclosure.

where c_0 is the speed of light, $W = 40$ cm, $L = 20$ cm, and $h = 50$ cm. The quantities $m, n,$ and p are integer valued mode indices.

Cross correlation, as defined in signal analysis (e.g., [3]), can be used to check the degree of similarity between two signals. In this case, the two signals will be defined as X_i consisting of 1600 equally-spaced frequency domain samples of $|S_{11}|$ expressed in decibels for the reference case (no thermal gasket material) and Y_i consisting of 1600 equally-spaced frequency domain samples of $|S_{11}|$ expressed in decibels for the dielectrically loaded patch. The cross correlation coefficient for these two signals will then be R_n where

$$R_n = \begin{cases} \frac{1}{N-|n|} \sum_{i=1}^{N-|n|} X_{i+n} Y_i \text{ for } n \geq 0 \\ \frac{1}{N-|n|} \sum_{i=1}^{N-|n|} Y_{i+n} X_i \text{ for } n < 0 \end{cases} \quad (4)$$

Figs. 5 and 6 show the cross-correlation coefficient with the frequency-shift index converted into gigahertz. Fig. 5 shows the cross correlation for the two curves shown in Fig. 2 (patch antenna structure in open space) while Fig. 6 shows the cross correlation for the two curves shown in Fig. 4 (patch-antenna structure in a slotted metal enclosure). In both cases, the peak cross-correlation coefficient seems to occur at a frequency shift of approximately -0.5 GHz. Of course, the cross correlation curve in the latter case is both more diffuse and more jagged since the S_{11} curve in this case contains individual enclosure resonances that are not significantly altered by the presence or absence of thermal gasket material. Nevertheless, the observed frequency shift is consistent in both cases and also agrees closely with the frequency shift suggested by a visual inspection of Fig. 2.

III. Frequency Shift versus Bandwidth

For the TM^z_{010} mode of the patch antenna, the resonant frequency is given by [4] as

$$(f_r)_{010} = \frac{c_0}{2(L + \Delta L)\sqrt{\epsilon_f}}. \quad (5)$$

The quantities ΔL and ϵ_f are both the results of intermediate calculations for the fringing field compensation. From [4], when the relative permittivity is replaced with the effective relative permittivity $(\epsilon_{r,\text{effective}})$ these additional quantities are given by

$$\Delta L = 0.412 \left[\frac{\epsilon_{r,\text{effective}} + 0.300}{\epsilon_{r,\text{effective}} - 0.258}\right] \left[\frac{\frac{L}{h} + 0.262}{\frac{L}{h} + 0.813}\right] \cdot h \quad (6)$$

$$\epsilon_f = \frac{\epsilon_{r,\text{effective}} + 1}{2} + \frac{\epsilon_{r,\text{effective}} - 1}{2} \left[1 + \frac{10h}{L}\right]^{-1/2} \quad (7)$$

where L and h are the length and height of the patch. For a patch antenna the bandwidth, the radiation quality factor Q_r, and the standing wave ratio (VSWR) for the mode are related by [4]

$$\text{BW} = \frac{\text{VSWR} - 1}{Q_r \sqrt{\text{VSWR}}}. \quad (8)$$

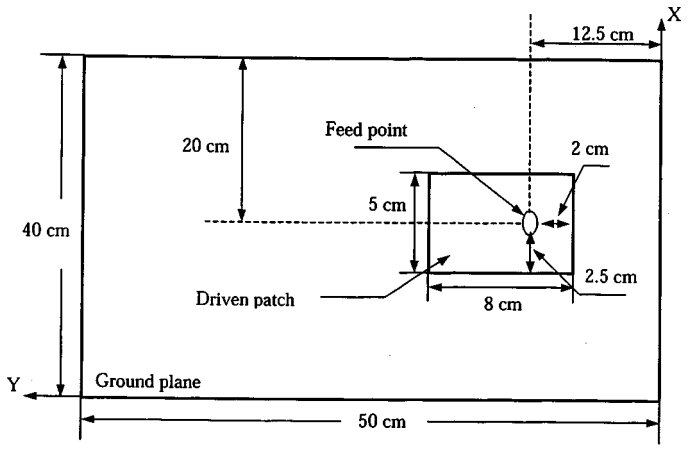

Fig. 7. Driven-patch dimensions for exciting the TM^{z}_{010} mode.

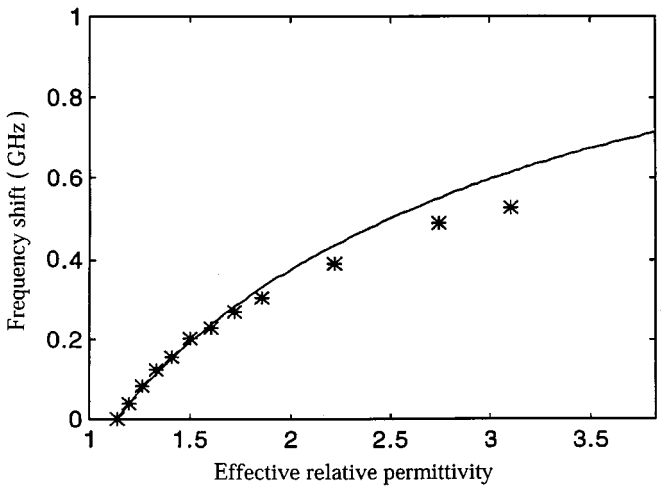

Fig. 8. Measured $(*)$ and calculated (solid line) values of the frequency shift as a function of the effective-relative permittivity.

The standing-wave ratio of the patch antenna, in turn, is related to the S_{11} parameter by

$$\mathrm{VSWR} = \frac{1 + |S_{11}|}{1 - |S_{11}|}. \tag{9}$$

Therefore, knowing the quality factor Q_r and specifying an acceptable value for either $|S_{11}|$ or VSWR allows the estimation of the fractional bandwidth. The quality factor for the TM^{z}_{010}-mode can be estimated by following the procedure described by Carver and Mink [4]

$$Q_r = \frac{\mathrm{Re} : \{k_{010}\}}{2 \times \mathrm{Im} : \{k_{010}\}} \tag{10}$$

where k_{010} is the complex eigenvalue associated with the propagation of the TM^{z}_{010}-mode. This eigenvalue is obtained as the iterative solution of a complex transcendental equation.

An additional set of experimental measurements was made to compare the calculated and experimental values of both the resonant frequency and the bandwidth of the TM^{z}_{010}-mode. By placing the feed point off center with respect to the long dimension of the patch, it was possible to excite the TM^{z}_{010}-mode. By placing the feed point in the center of the short dimension, it was possible to suppress the TM^{z}_{100}-mode. The geometry of the patch antenna source used in this set of measurements is shown in Fig. 7. Fig. 8 is a comparison of the numerically predicted frequency shift and the measured frequency shift. The reference case for this figure was a patch antenna structure with a 3.8-mm thick cardboard spacer and therefore a zero-frequency shift in this case occured by definition at $\epsilon_{r,\mathrm{effective}} = 1.15$ rather than $\epsilon_{r,\mathrm{effective}} = 1.00$.

As an example of the calculated bandwidth, Fig. 9 shows a small portion of the S_{11} curve. The -3-dB bandwidth for the magnitude of S_{11} corresponds to a measured bandwidth of approximately 0.157 GHz on Fig. 9. Substituting (9) and (10) into (8) while using (5) to convert from normalized bandwidth to bandwidth in gigahertz, yields a calculated bandwidth of 0.15 GHz.

Based on the calculated values of the resonant frequency and bandwidth for the TM^{z}_{010}-mode, a table was constructed to show

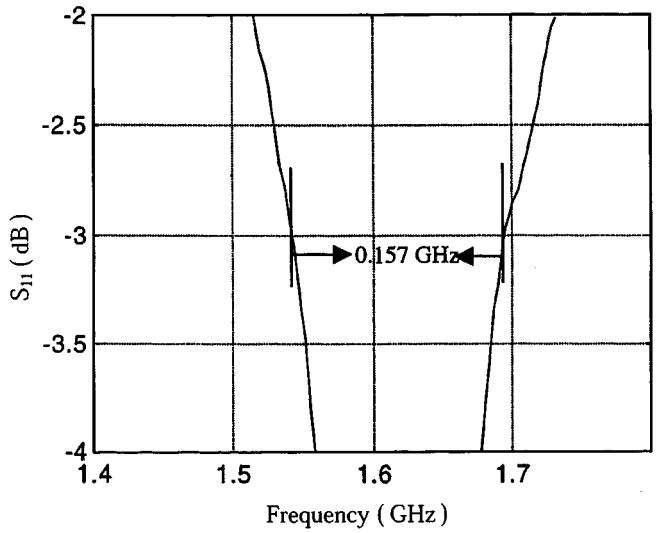

Fig. 9. -3-dB bandwidth of an 8 by 5 cm by 3.81 mm patch antenna TM^{z}_{010}-mode.

how changes in the effective relative permittivity result in various frequency shift to bandwidth ratios. Specifically, the rows of Table I correspond to the old values of effective relative permittivity and the columns correspond to the new values of the effective relative permittivity. Entries in the top row denote the effective relative permittivity of the new material while entries in the first column denote the effective relative permittivity of the old material. The specific values of effective relative permittivity were chosen to match the effective relative permittivities of a number of available test materials.

The remaining entries in this table consist of frequency shift to bandwidth ratios. Thus, for example, in going from an effective relative permittivity of $\epsilon_{r\,\mathrm{old}} = 1.14$ to an effective relative permittivity of $\epsilon_{r\,\mathrm{new}} = 1.86$ the frequency shift to bandwidth ratio of -1.99 denotes that the resonant frequency of the TM^{z}_{010}-mode has been lowered by 1.99 times the bandwidth. The bandwidth in this context is defined as the frequency interval in gigahertz between the -3-dB points in the S_{11} curve

TABLE I
CALCULATED VALUES OF THE FREQUENCY SHIFT TO BANDWIDTH RATIO.

	ϵ_{rnew} = 1.14	ϵ_{rnew} = 1.26	ϵ_{rnew} = 1.41	ϵ_{rnew} = 1.60	ϵ_{rnew} = 1.86	ϵ_{rnew} = 2.74
ϵ_{rold} = 1.14	0.00	-0.53	-1.01	-1.50	-1.99	-3.19
ϵ_{rold} = 1.26	0.53	0.00	-0.54	-1.08	-1.62	-2.95
ϵ_{rold} = 1.41	1.01	0.54	0.00	-0.60	-1.21	-2.71
ϵ_{rold} = 1.60	1.50	1.08	0.60	0.00	-0.71	-2.49
ϵ_{rold} = 1.86	1.99	1.62	1.21	0.71	0.00	-2.02
ϵ_{rold} = 2.74	3.19	2.95	2.71	2.49	2.02	0.00

(see Fig. 9 for an example). It should be noted, however, that replacing the dielectric material, generally changes both the resonant frequency and bandwidth of the mode. The data shown in this table use the wider of the old and new bandwidths. Generally, this means that when the frequency shift is positive (the new material has a smaller effective relative permittivity) the frequency shift to bandwidth ratio uses the bandwidth associated with the new material. When the frequency shift is negative, the bandwidth associated with the old material is used.

Table II presents the corresponding measured results in the same format. One of the possible sources of disagreement between the results in Tables I and II reflects the uncertainty in determining the relative permittivity [5]. The relative permittivity values were determined experimentally with both custom built-test fixtures and a commercial material analyzer. The differences in the results of Tables I and II are commensurate with the uncertainties in the relative permittivity.

IV. DESIGN GUIDELINES

The purpose of the design guidelines is to indicate how much the resonant frequency of the TM^{z}_{010}-mode will be shifted as the effective relative permittivity of the dielectric material in the patch antenna is changed from an old value to a new value. These guidelines are based upon numerical calculation for a simplified model of a patch source operating in the lowest order mode (TM^{z}_{010}).

As a first step, a table of frequency shift to bandwidth ratios was again calculated for a patch source measuring 5 by 8 cm with a thickness of 0.38 cm. The effective relative permittivities in this case ranged from 1 to 4 in steps of 0.5. The data in the table were used to construct a graphical-design guideline in the form of a contour plot as shown in Fig. 10. Starting with a heat-sink gasket material having an effective relative permittivity of 2.0, for example, this figure shows that the resonant frequency of the TM^{z}_{010} could be shifted downward by three times the bandwidth if the heat sink material is replaced with a new material having an effective relative permittivity of approximately 3.2 as denoted by the small open circle in this figure. A similar procedure can be used to develop graphical design charts for heat sinks having different dimensions.

V. SUMMARY AND CONCLUSION

Ultimately, the primary criterion in selecting thermal gasket materials is their thermal characteristics. However, given a choice of two or more materials having similar thermal characteristics, the EMI considerations addressed in the design guidelines may be useful in mitigating radiated emissions based on the resonant frequency shifting effect of nonconductive materials placed in patch-antenna sources. The patch-antenna source was used as a simplified model for the mechanism of radiated emissions attributed to poorly grounded heat sinks. Simple cavity-resonance models of the patch antenna sources were used to predict the resonant frequencies and these predictions generally agreed with measured values when the patch antenna source was located in the shielded room test site. However, when the patch source was placed inside

TABLE II
EXPERIMENTALLY DETERMINED VALUES OF THE FREQUENCY SHIFT TO BANDWIDTH RATIO

	ϵ_{rnew} = 1.14	ϵ_{rnew} = 1.26	ϵ_{rnew} = 1.41	ϵ_{rnew} = 1.60	ϵ_{rnew} = 1.86	ϵ_{rnew} = 2.74
ϵ_{rold} = 1.14	0.00	-0.41	-0.86	-1.35	-1.89	-3.15
ϵ_{rold} = 1.26	0.41	0.00	-0.52	-1.08	-1.70	-3.14
ϵ_{rold} = 1.41	0.86	0.52	0.00	-0.66	-1.38	-3.07
ϵ_{rold} = 1.60	1.35	1.08	0.66	0.00	-0.86	-2.88
ϵ_{rold} = 1.86	1.89	1.70	1.38	0.86	0.00	-2.49
ϵ_{rold} = 2.74	3.15	3.14	3.07	2.88	2.49	0.00

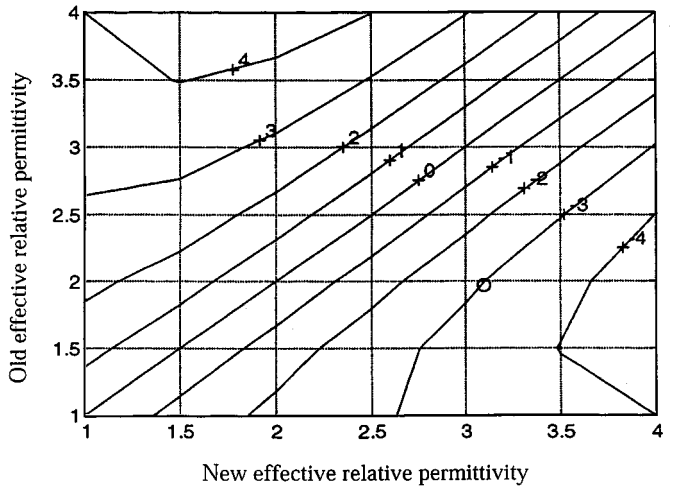

Fig. 10. Contour plot of the frequency shift to bandwidth ratio for a heat sink measuring 8 cm by 5 cm by 3.81 mm.

a slotted metal enclosure, having dimensions comparable with a personal computer or workstation chassis, the resonant frequencies of the patch antenna were obscured by the presence of resonant modes due to the enclosure. These enclosure modes made it difficult to compare the frequency shifting effects of various materials placed in the patch antenna. For this reason, a cross-correlation technique was developed. After applying this data-analysis tool, the frequency shift produced by loading the patch antenna source with various nonconductive materials was found to be comparable regardless of whether the patch source was in an enclosure or in free space.

In order to be useful as a radiated-emissions reduction strategy, it is necessary for the frequency shift to be significant when compared to the bandwidth of the patch-antenna resonance. Therefore, experimental measurements of the frequency shift to bandwidth ratio were made. Numerical predictions of the frequency shift to bandwidth ratio were also made for the dominant (lowest frequency) mode. The predicted and measured ratios generally agreed well (within 30% for most cases). Therefore, the numerical predictions can be used to generate a set of design guidelines for heat sinks of various sizes.

It should be emphasized that changing heat-sink gasket materials as an EMI mitigation strategy is limited to cases in which the heat-sink patch resonance constitutes a significant part of the overall coupling mechanism. Even then, it is necessary to ensure that the shifted patch-resonance frequency does not coincide with a clock harmonic. Despite these limitations, there are at least two commercial products in which the substitution of one electrically insulating heat sink gasket for another (of the same size but different composition) has resulted in significantly reduced radiated EMI at certain troublesome frequencies. In one of these cases, this reduction was sufficient to allow the product to meet FCC requirements.

REFERENCES

[1] S. Radu, Y. Ji, J. Nuebel, J. L. Drewniak, T. P. Van Doren, and T. H. Hubing, "Identifying an EMI source and coupling path in a computer system with sub-module testing," in *Proc. IEEE Electromagnetic Compatibility Symp.*, Austin, TX, 1997, pp. 165–170.

[2] J.-F. Zurcher and F. E. Gardiol, *Broadband Patch Antennas*. Norwood, MA: Artech House, 1995.

[3] A. Papoulis, *Random Variables and Stochastic Processes*, 2nd ed. New York: McGraw-Hill, 1984.

[4] K. R. Carver and J. W. Mink, "Micro antenna technology," *IEEE Trans. Antennas Propagat.*, vol. AP-29, pp. 2–24, Jan. 1981.

[5] Y. Huang, "Numerical and Experimental Studies of EMI Reduction Through the Use of Thin Conductive and Nonconductive Materials," Master's thesis, Dept. of Elect. Eng., Univ.of Missouri-Rolla, Rolla, MO, 1999.

Yu Huang received the B.S. degree from Tsinghua University, Beijing, China, in 1997, and the M.S. degree from University of Missouri, Rolla, in 1999, both in electrical engineering. She is currently working toward the Ph.D. degree in computer science at the University of Washington, Seattle.

From 1997 to 1999, she was a Research Assistant in the EMC Laboratory at the University of Missouri. She is now a Software Engineer with the AOL Wireless Division, Seattle, WA.

Joseph E. Butler (M'75–SM'90) received the B.S. degree in engineering physics from Merrimack College, North Andover, MA, in 1967, the M.A. degree in physics from Williams College, Williamstown, MA in 1969, and the M.B.A. degree from Northeastern University, Boston, MA in 1974.

From 1969 to 1971 he was an EMC Engineer for RCA Aerospace Systems Division, Burlington, MA, and in a similar position with Raytheon Company Missile Systems Division, Bedford, MA, from 1971to 1980. From 1980 to 1986 he was the Manager of Corporate Standards for GenRad, Concord, MA. Since 1986, he has been with the Chomerics Division of Parker Hannifin Company, Woburn, MA, where he is currently a Senior Electromagnetic Compatibility Consultant and Marketing Manager involved with new product development and new technology investigations. His new product development activities involve emerging EMI gasket technologies.

Mr. Butler is president of the IEEE EMC Society for the two-year term 2000–2001.

Miksa de Sorgo (M'94) received the B.S.degree in chemistry, from John Carroll University, Cleveland, OH, in 1963, and the Ph.D. degree in physical chemistry, from the University of Alberta, Edmonton, Canada, in 1968.

He was a postdoctoral Fellow at the SUNY College of Forestry, Syracuse, NY, from 1969 to 1971, and a Chemistry Research Associate at Syracuse University, Syracuse, NY, from 1971 to 1972. From 1972 to 1977, he was a Senior Research Chemist at the SCM Corporation, Cleveland, OH, where he worked in the field of polymer coatings. From 1977 to 1981, he was a New Products Development Manager at Mobil Chemical Company, Edison, NJ. He joined Chomerics in 1981, now a division of Parker Hannifin Corporation, Woburn, MA, where he presently holds the position of Principal R & D Scientist. He is actively involved in the development of materials for the thermal management of electronic components and the development of standards for the measurement of material thermal properties.

Dr. de Sorgo is a member of ASTM and IMAPS.

Richard E. DuBroff (S'74–M'77–SM'84) received the B.S.E.E. degree from Rensselaer Polytechnic Institute, Troy, NY, in 1970, and the M.S. and Ph.D. degrees in electrical engineering from the University of Illinois, Urbana-Champaign, in 1972 and 1976, respectively.

From 1976 to 1978, he held a postdoctoral position in the Ionosphere Radio Laboratory, University of Illinois, Urbana-Champaign, and worked on backscatter inversion of ionospheric electron density profiles. From 1978 to 1984, he was a Research Engineer in the geophysics branch of Phillips Petroleum, Bartlesville, OK. Since 1984, he has been affiliated with the University of Missouri, Rolla where he is currently a Profesor in the Department of Electrical and Computer Engineering.

Todd H. Hubing (S'82–M'82–SM'93) received the B.S.E.E. degree from the Massachusetts Instituyte of Technology, Cambridge, in 1980, the M.S.E.E. degree from Purdue University, West Lafayette, IN, in 1982, and the Ph.D. degree in electrical engineering from North Carolina State University, Raleigh, NC, in 1988.

He is currently a Professor of electrical engineering at the University of Missouri, Rolla where he is also a member of the principal faculty in the Electromagnetic Compatibility Laboratory. Prior to joining the faculty at the University of Missouri-Rolla in 1989, he was an Electromagnetic Compatibility Engineer at IBM, Research Triangle Park, NC. He has authored or presented more than 70 technical papers, presentations, and reports on electromagnetic modeling and electromagnetic compatibility-related subjects. He also writes the satirical "Chapter Chatter" column for the IEEE EMC SOCIETY NEWSLETTER. Since joining the UMR, the focus of his research has been measuring and modeling sources of electromagnetic interference.

Dr. Hubing is on the Board of Directors for the IEEE EMC Society.

James L. Drewniak (S'85–M'90) received the B.S. (highest honors), M.S., and Ph.D. degrees in electrical engineering, all from the University of Illinois, Urbana-Champaign, in 1985, 1987, and 1991, respectively.

In 1991, he joined the Electrical Engineering Department at the University of Missouri, Rolla, where he is a Professor and is affiliated with the Electromagnetic Compatibility Laboratory. His research interests include the the development and application of numerical methods for investigating electromagnetic compatibility problems, packaging effects, and antenna analysis, as well as experimental studies in electromagnetic compatibility and antennas.

Thomas P. Van Doren (S'60–M'69–SM'96) received the B.S., M.S., and Ph.D. degrees from the University of Missouri, Rolla in 1962, 1963, and 1969, respectively.

From 1963 to 1965, he served as an Officer in the U. S. Army Security Agency. From 1965 to 1967, he was a Microwave Engineer with Collins Radio Company, Dallas, TX. Since 1967, he has been a member of the electrical engineering faculty at the University of Missouri, where he is currently a Professor. His research interests concern developing circuit layout grounding, and shielding techniques to improve electromagnetic compatibility. He has taught short courses on electromagnetic compatibility to over 10 000 engineers and technicians representing 200 corporations.

Dr. Van Doren received the IEEE EMC Society Richard R. Stoddard Award for his contributions to electromagnetic compatibility research and education in 1995. He is a Registered Professional Engineer in the state of Missouri and a member of Eta Kappa Nu, Tau Beta Pi, and Phi Kappa Phi.